Chapter 21
Monitoring of Spatiotemporal Dynamics of Rabi Rice Fallows in South Asia Using Remote Sensing

Murali Krishna Gumma, Prasad S. Thenkabail, Pardhasaradhi Teluguntla, and Anthony M. Whitbread

Abstract Cereals and grain legumes are the most important part of human diet and nutrition. The expansion of grain legumes with improved productivity to cater the growing population's nutritional security is of prime importance and need of the hour. Rice fallows are best niche areas with residual moisture to grow short-duration legumes, thereby achieving intensification. Identifying suitable areas for grain legumes and cereal grains is important in this region. In this context, the goal of this study was to map fallow lands followed by rainy season (*kharif*) rice cultivation or post-rainy (*rabi*) fallows in rice-growing environments between 2005 and 2015 using temporal moderate-resolution imaging spectroradiometer (MODIS) data applying spectral matching techniques. This study was conducted in South Asia where different rice ecosystems exist. MODIS 16 day normalized difference vegetation index (NDVI) at 250 m spatial resolution and season-wise-intensive ground survey data were used to map rice systems and the fallows thereafter (*rabi* fallows) in South Asia. The rice maps were validated with independent ground survey data and compared with available subnational-level statistics. Overall accuracy and kappa coefficient estimated for rice classes were 81.5% and 0.79%, respectively, with ground survey data. The derived physical rice area and irrigated areas were highly correlated with the subnational statistics with R^2 values of 94% at the district level for the years 2005–2006 and 2015–2016. Results clearly show that rice fallow areas increased from 2005 to 2015. The results show spatial distribution of rice fallows in South Asia, which are identified as target domains for sustainable intensification of short-duration grain legumes, fixing the soil nitrogen and increasing incomes of small-holder farmers.

Keywords Grain legumes · Ground survey data · MODIS 250 m · NDVI · Potential areas · Seasonal rice mapping · Rice fallows · Spectral matching techniques

M. K. Gumma (✉) · A. M. Whitbread
International Crops Research Institute for the Semi-Arid Tropics, Patancheru, Hyderabad, India
e-mail: M.Gumma@cgiar.org

P. S. Thenkabail · P. Teluguntla
U.S. Geological Survey (USGS), Western Geographic Science Center, Flagstaff, AZ, USA

© Springer International Publishing AG, part of Springer Nature 2018

G. P. O. Reddy, S. K. Singh (eds.), *Geospatial Technologies in Land Resources Mapping, Monitoring and Management*, Geotechnologies and the Environment 21,
https://doi.org/10.1007/978-3-319-78711-4_21

21.1 Introduction

Agriculture is the key to food security and nutrition for the growing populations of Asia and Africa improving incomes and employment. We need to produce at least 50% more to feed the projected 9.15 billion people by 2050 (Alexandratos and Bruinsma 2012). Agricultural and rural development are critical to the eradication of poverty and improvement livelihoods for sustainable and equitable growth. There is a need to increase cropping intensity (two to three crops within a crop year) where there is no scope for extensification in most of South Asia, which is known as food bowl of the world, with 60 million ha planted with rice. South Asia accounts for 40% of the world's harvested rice area (USDA 2010) and almost 25% of the world's population (FAO 2015). Rice is grown under irrigated and rainfed conditions in various ecosystems in South Asia. In most irrigated rice-grown areas, rice followed by rice, rice followed by wheat, rice followed by mustard, and rice followed by pulses are the regular practice. Major rice-growing area under rainfed conditions and followed by fallow is mainly located in the eastern part of India, Bangladesh, and Sri Lanka (Gumma et al. 2011b). Growing food demand has increased pressure to intensify existing croplands with increased use of irrigation technology, fertilizer, and mechanization (Garnett et al. 2013; Gray et al. 2014). Information on existing rice systems is important to intensify with short-duration grain legumes and dryland cereals.

Monitoring irrigated croplands, rainfed croplands, crop intensity, and land-use changes spatially is critical for planning agriculture development and sustainable food production. Spatial information is very important for prioritizing based on environmental and social factors and also where we could target short-duration crops (Gumma et al. 2014). Remote sensing is the ideal tool and provides an alternative, quick, and independent approach to estimate cropland extent seasonally and crop intensity over large areas (Gumma et al. 2011a; Gumma et al. 2016; Subbarao et al. 2001) and changes in croplands of a country (Badhwar 1984; Lobell et al. 2003; Thenkabail 2010; Thiruvengadachari and Sakthivadivel 1997). Many researchers worked on spatiotemporal analysis to map agriculture areas by irrigation source (Gumma et al. 2011c, d, 2015a; Knight et al. 2006; Thenkabail et al. 2005, 2007; Velpuri et al. 2009), specific crop-type mapping and temporal changes (Gumma et al. 2015b; Gumma et al. 2014), and crop intensity (Gumma et al. 2014; Sakamoto et al. 2005). Several studies have mapped rice areas with optical and synthetic-aperture radar (SAR) imagery. The number of studies have been conducted with MODIS time series data applying various methods. NDVI was widely used to map rice areas (Gumma et al. 2011b). Land surface water index (LSWI) and enhanced vegetation index (EVI) derived from temporal MODIS data were also used to map rice areas (Sakamoto et al. 2005; Shao et al. 2001). Spectral matching techniques were widely used to map irrigated areas, land use/land cover

(LULC), and rice crop mapping (Biradar et al. 2009; Gumma et al. 2015a; Thenkabail et al. 2007, 2009).

Given the above background, this paper mapped the fallow lands followed by rainy season (*kharif*) rice cultivation or post-rainy (*rabi*) fallows in rice-growing environments between 2000 and 2015. Accurate and up-to-date information on the spatial distribution of rice fallows is widely recognized as very important domain to target short-duration grain legumes. The aim of this research was to map rice fallows in South Asia as derived initially by mapping cropland extent by irrigation source and different rice systems using MODIS 16 day interval time series imagery for the years 2005–2006 to 2014–2015 applying spectral matching technique, phenological approaches, and intensive ground survey information.

21.2 Study Area

South Asia is located between 5°38′40″ and 36°54′30″ latitudes and 61°05′00″ and 97°14′15″ longitudes, with total geographical area of 477 Mha (Fig. 21.1). It has six agroecological zones: humid tropics, subhumid tropics, semiarid tropics, semiarid, subtropics, and arid (Choice 2009). South Asia is surrounded by Western Asia, Central Asia, East Asia, Southeast Asia, and the Indian Ocean. It includes six countries, Pakistan, India, Nepal, Bhutan, Bangladesh, and Sri Lanka. In South Asia, 80% of poor live in rural areas, and they mostly depend on agriculture for their livelihood (World Bank 2015). Nine major river basins were included in the study area: the Indus, Ganges, Brahmaputra, Narmada, Tapti, Godavari, Krishna, Kaveri, and Mahanadi. There are many major and minor irrigation projects in South Asia, covering a total command area of 133 Mha (Thenkabail et al. 2008). However, the ultimate potential is 139 m.ha, the increase being primarily due to upward revision in assessed potential of minor groundwater schemes and minor surface water schemes to 64 m.ha and 17 Mha, respectively. Rice is the major crop in this region, and it is grown two times a year in the entire region, but Bangladesh grows it three times a year (Table 21.1).

21.3 Data and Methods

The methodology for the identification of land-use changes and targeting of new technologies is shown in Fig. 21.2 and is described in the following sections.

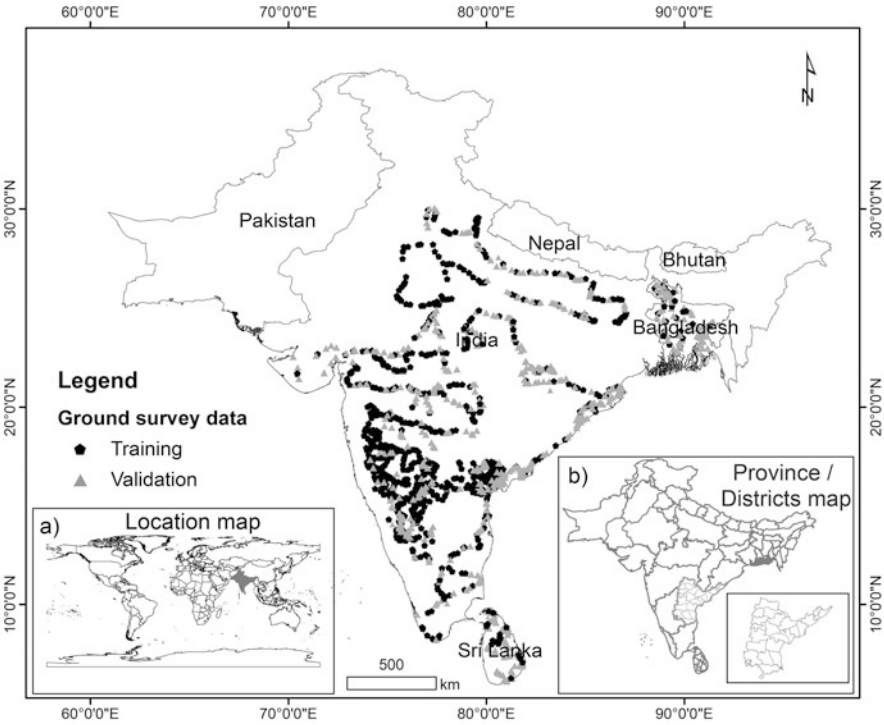

Fig. 21.1 Study area with countries and district boundaries. (**a**) Location map shown in the world and (**b**) administrative boundaries

Table 21.1 Country area and agricultural area in South Asia for 2010–2011

Country	Total geographical area ('000 ha)	Total gross planted area ('000 ha)	Net irrigated areas (NAS) ('000 ha)	Harvested area of rough rice (NAS) ('000 ha)
Bangladesh	14,804	15,002	6749	10,801
Bhutan	4365	121	27	26
India	3,45,623	1,84,443	63,601	44,712
Nepal	16,210	4208	1926	1560
Pakistan	89,167	22,817	19,270	2377
Sri Lanka	6453	2076	462	832
Total	4,76,622	2,28,668	92,035	60,308

Source: World Rice Statistics, FAO

21.3.1 Satellite Data and Processing

The present study used MOD13Q1.005 product, which provides 16 day composite images at 250 m spatial resolution. MOD13Q1.005 product includes vegetation indices, blue, red, and near-infrared (NIR) and mid-infrared (MIR) bands. Twelve

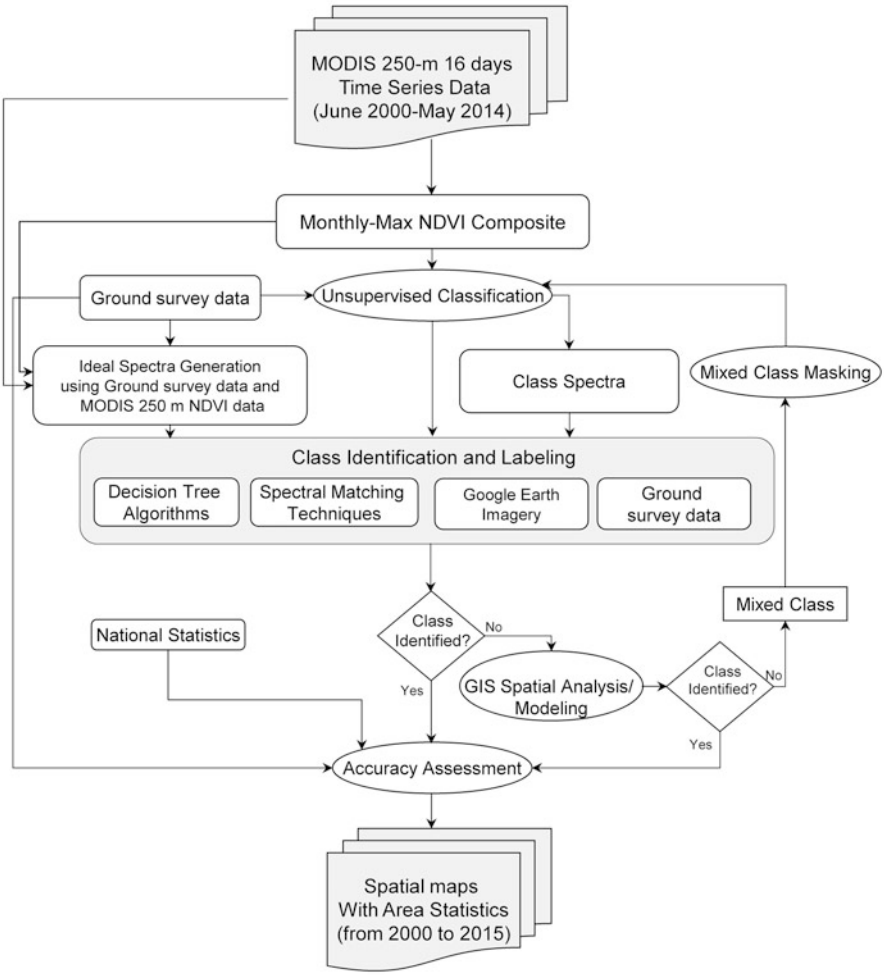

Fig. 21.2 Overview of the methodology for mapping rice fallows (rabi fallows) from 2000 to 2015 (each crop year)

tiles covering the South Asian region were downloaded from the Land Processes Distributed Active Archive Center (LP DAAC) (*https://lpdaac.usgs.gov*) (LPDAAC 2014). MODIS re-projection tool (MRT) was used to re-project and mosaic twelve tiles of study area and then stack them as single composite (Gumma et al. 2011b; Thenkabail et al. 2009). Altogether 23 images were stacked for the crop year from 2000 to 2015 (start from June to May).

$$\text{NDVIMVC}_i = \text{Max}(\text{NDVI}_{i1}, \text{NDVI}_{i2}) \tag{21.1}$$

where MVC_i is monthly maximum-value composite of i^{th} month (e.g., "i" is Jan–Dec) and i_1 and i_2 are every 16 day composite in a month. The NDVI data was

further processed to create monthly maximum-value composites (MVC) for each of the crop year using Eq. 21.1.

21.3.2 Ground Survey Information

Ground survey information was collected at different times for three distinct projects, which could be collectively used to increase the sample size for class identification as well as accuracy assessment (Fig. 21.1). The first set of field points (996 locations) were collected during October 2003 and September 2005 for mapping irrigated areas, and the second set of field-plot dataset (402 locations) were collected during August and September 2010. At each point, information was collected on existing crop type and soil type and LULC information at 250 m × 250 m plot along with geographical coordinates using a handheld GPS unit. Crop type and irrigation type were collected during the survey. During the collection of such points under irrigated conditions, the area surrounding the point is categorized into three classes, small ($\leq$10 ha), medium (10–15 ha), and large ($\geq$15 ha), in which "small" category means that $\leq$10 ha of irrigated area is present around the surveyed point. Also additional information was gathered through interviews with farmers and district agricultural officers to determine crop intensities and crop type during the previous year. A total of 830 locations covering the major cropland areas were chosen based on the knowledge of district agricultural extension officers to ensure adequate samples of major crops as well as other LULC information along with two photographs from each location. The remaining 568 points were only the geographic coordinates, cropping pattern/intensity by landholding size. The farmers provided information on crop calendars, cropping intensity (single or double crop), and percentage canopy cover for these locations. The interview included a question on planting dates, irrigation type, and cropping pattern. Ground survey information samples were based on local expert knowledge, distinct LULC type, and preliminary land-use classification. Some important irrigated areas were not visited due to road conditions and time constraints. Information was obtained in these areas from agriculture and irrigation departments. LULC names of class labels were assigned in the field using a labeling protocol (Gumma et al. 2014).

21.3.3 Ideal Spectra Signatures

Ideal spectra signatures were generated using 16 day NDVI time series composite and precise ground survey information, which was also used for class identification process (Fig. 21.3) (Gumma et al. 2016). Ideal spectral signatures were based on 303 ground survey information; these samples were grouped according to their unique categories and grouped major rice systems as shown in Fig. 21.3. Ideal spectra signatures were generated by considering crop intensity, crop type, and

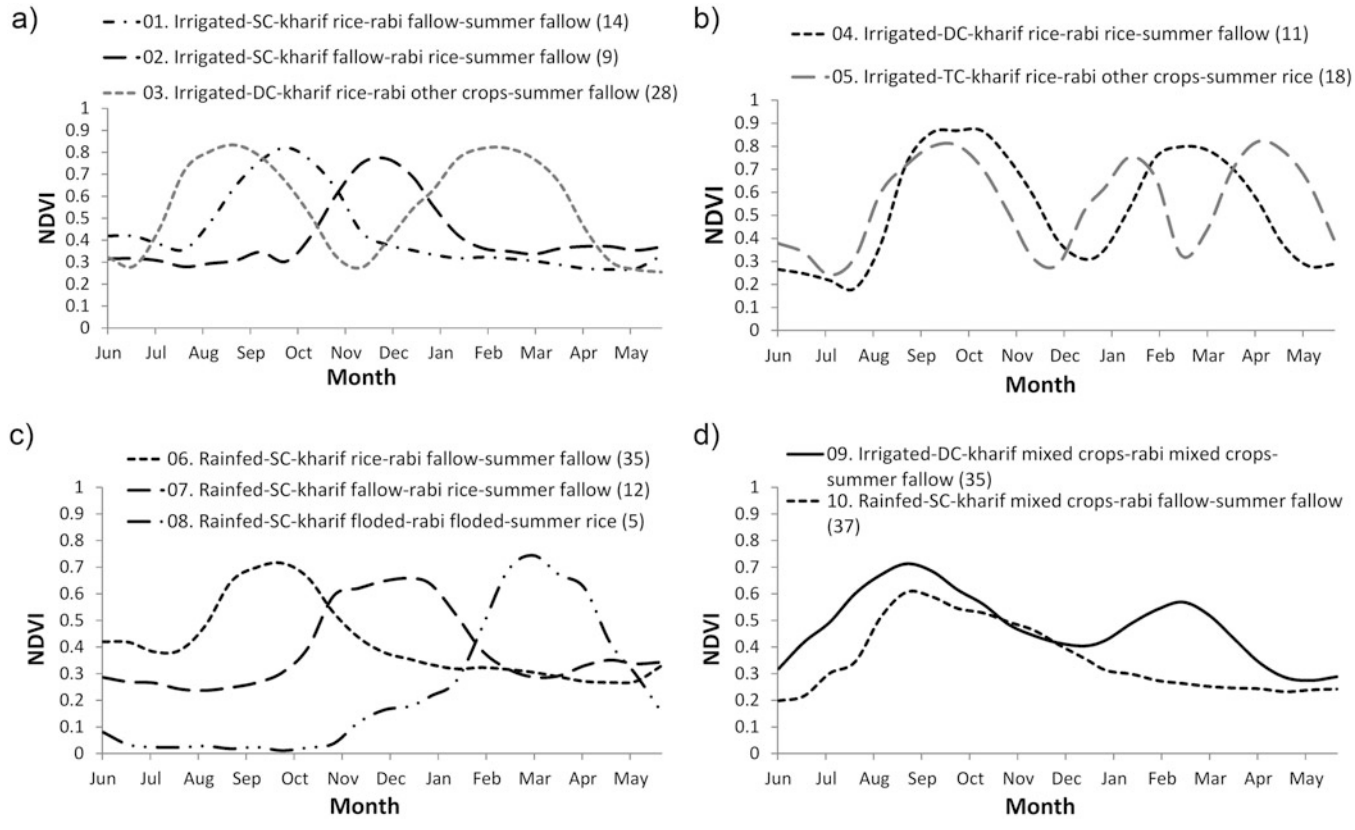

Fig. 21.3 Ideal spectra signatures. (**a**) Irrigated rice: (01) kharif (June–October) irrigated rice, rabi fallow; (02) rabi (November–February) irrigated rice, kharif fallow; (03) summer (March–May) irrigated rice, kharif and rabi fallow. (**b**) Irrigated rice: (04) kharif irrigated rice, rabi irrigated rice, summer fallow; (05) kharif irrigated rice, rabi fallow, summer rice. (**c**) Rainfed rice: (06) kharif rainfed rice, rabi, and summer fallow; (07) kharif fallow, rabi rice, summer fallow; (08) kharif and rabi fallow, summer rice; (09) kharif-mixed crops, rabi-mixed crops, summer fallow; (10) kharif-mixed crops, rabi fallow, summer fallow (Gumma et al. 2016)

cropping systems. Each signature was generated with group of similar samples. For example, Fig. 21.3a, class 1 "01. Irrigated single crop rice fallow (14)" signature defines irrigated as during kharif season followed rabi and summer fallows, and this was generated by 14 ground survey sample temporal information. Finally, eight rice spectra profiles were aggregated from the 132 sample locations.

21.3.4 Rice Classification

The generation of ideal spectra using time series imagery at selected ground survey points is the primary step in class identification. Ground survey points were chosen region-wise representing specific crop type, length of growing period (planting and harvesting), and irrigation source. Each ideal spectrum was generated by using 10–15 samples for each region (Gumma et al. 2011b; Gumma et al. 2014; Gumma et al. 2016; Thenkabail et al. 2007). Unsupervised classification using ISOCLASS cluster algorithm (ISODATA in ERDAS Imagine 2014™) followed by progressive generalization (Cihlar et al. 1998) was applied on MODIS 250 m 16 day composite NDVI for the crop year 2010–2011. The initial classification was set at a maximum of 100 iterations and a convergence threshold of 0.99. Initially 15 classes were extracted from unsupervised classification.

Class spectra were generated using ISOCLASS *k*-means classification using MODIS composite (Tou and Gonzalez 1975). The signatures were plotted for each LULC over time (Gumma et al. 2011b). Initial classes were grouped to ten using decision tree algorithm (Dheeravath et al. 2010; Gumma et al. 2011b, d). Decision tree rules are based on NDVI thresholds at different stages in the vegetation growth cycle, and this algorithm helps to identify similar classes. Rules were also based on field knowledge of particular locations from ground survey information. After initial grouping of classes, further grouping of similar classes was based on spectral matching techniques (SMT) (Homayouni and Roux 2003; Thenkabail et al. 2007). Temporal profiles of each group of classes were further compared with the ideal spectra in order to identify and name the class accurately. Additional verification was conducted using high-resolution imagery from Google Earth and GeoCover by overlaying district administrative boundaries in the Google Earth application. Mixed classes remained because of the large extent and diverse land use in small holdings. For resolving these mixed classes, we used various other sources such as irrigation command area boundaries, rainfall, district-level statistics, and high-resolution imagery using spatial modeling (Gumma et al. 2014). Some rare classes may not resolve conclusively even after using ground survey information. These classes were subset from the initial time series stack, and the above protocols were applied on this subset for class identification.

21.3.5 Rice Fallow Identification

The NDVI plots are ideal for understanding the changes within and between cropping seasons and between classes and exhibits the length of growing period. Temporal NDVI signature clearly elicits the planting time, peak growth, and harvesting stage in Fig. 21.3. Figure 21.3 also illustrates how the NDVI gradually goes up during the middle of July and reaches a peak (0.7) in October and gradually comes down to become a flat line indicating the cultivation of *kharif* rice followed by fallow.

NDVI time series plays a major role in class identification and determining crop growth stages season wise. Separation of rice-growing areas from other land-use/land cover classes is based on annual average NDVI values and timing of the onset of "greenness." The annual NDVI of double-cropped and triple-cropped rice areas was higher than the other crops; meanwhile, the difference between irrigated and rainfed rice areas is also clearly seen in the study area.

The dates of vegetation transitions were determined using the NDVI time series and a double-logistic model of vegetation phenology (Biggs et al. 2006; Fischer 1994):

$$\mathrm{NDVI}_t = v_s + \frac{k}{1+\exp(-c(t-p))} - \frac{k+v_s-v_e}{1+\exp(-d(t-q))} \tag{21.2}$$

where v_s is the starting of rice-growing season, v_e is the ending of rice-growing season, k is an asymptotic maximum value of NDVI, c and d are the slopes of the NDVI time series at the inflection points, and p and q are the dates of the inflection points (Fig. 21.3). The starting of the time series was defined as the date of minimum (boro rice), which starts in February and harvested in May. In the present study, we used physical comparison of individual class signatures with ideal spectra of crop. All classes were quantified with NDVI signatures and cropping calendars of each crop classes.

21.3.6 Area Calculation and Accuracy Assessment

MOD13Q1.005 pixel covers 250 m a side, and its area is 6.25 hectares; this is larger than many different crop fields in South Asia. Due to large pixel area, there is a possibility of diverse crops except rice crops because this crop is grown in large areas (Tungabhadra, Nagarjuna Sagar, and delta areas). This study was classified at 250 m spatial resolution; it is necessary to calculate subpixel areas to get actual LULC areas. We used ground survey points to generate subpixel areas; however, ground information observations include a visual estimation of LULC percentages at 250 m × 250 m (each point) during ground survey. Considering the fall of ground survey points in each LULC class will help in estimating the subpixel area for each

class based on average cropland area. This SPA crop fraction was applied to each land-use class and estimates net cropland areas and irrigated areas for study area with other LULC fractions in crop dominance classification.

Accuracy assessment was conducted on both resultant irrigated areas and rice maps (Congalton 2001; Jensen 2004), which generates an error matrix and accuracy map. Accuracy assessment was performed with 575 independent ground survey data. These data points were not used in class identification and labeling process.

21.3.7 Comparison with National Data

The final resultant irrigated subpixel area and subpixel rice areas generated from present study were compared against district-wise national statistics, such as irrigated area statistics adopted from Indiastat (www.indiastat.com) (INDIASTAT 2015). Rice statistics for India were obtained from the website of the Ministry of Agriculture's Directorate of Rice Development (http://dacnet.nic.in/rice/) and, for Bangladesh, Nepal, Pakistan, and Bhutan, from the national statistical departments. Irrigated area statistics were compared at province/state level (62 administrative units) and rice area compared at subdistrict level (812 administrative units).

21.4 Results and Discussion

21.4.1 Spatial Distribution of Croplands in South Asia

A typical agricultural landscape can be seen in the South Asian region (Fig. 21.4) for crop year 2015–2016. Most of the rainfed crops are spread over the Deccan Plateau, and irrigated cropping is prevalent mostly along the river courses. The rainfed cropped areas grown during the southwest monsoon are mostly highlands limited by water availability. Irrigated areas occur extensively and are concentrated in deltas and command areas of major river basins, such as Indo-Ganges, Godavari, Krishna, and Kaveri. Groundwater-irrigated areas are located across the study regions and mostly located in India. Figure 21.4 illustrates five irrigated classes, in which class 3 is irrigated by groundwater (GW) with double crop (DC), class 4 is irrigated by canal (surface water) with continuous crops, and classes 5 and 6 are irrigated by surface water (SW) with triple-cropped and single-cropped areas, respectively. Canal-irrigated double crops were located in headenders of command areas, and single-cropped areas were located at the tailenders. Rainfed areas were located outside of command areas and mainly located in the central part of India and uplands. The resultant class names (Fig. 21.4, Table 21.2) are based on dominance of particular land cover with in the irrigated areas. Table 21.2 shows area under different irrigated classes along with other LULC areas estimated with full pixel areas (FPA).

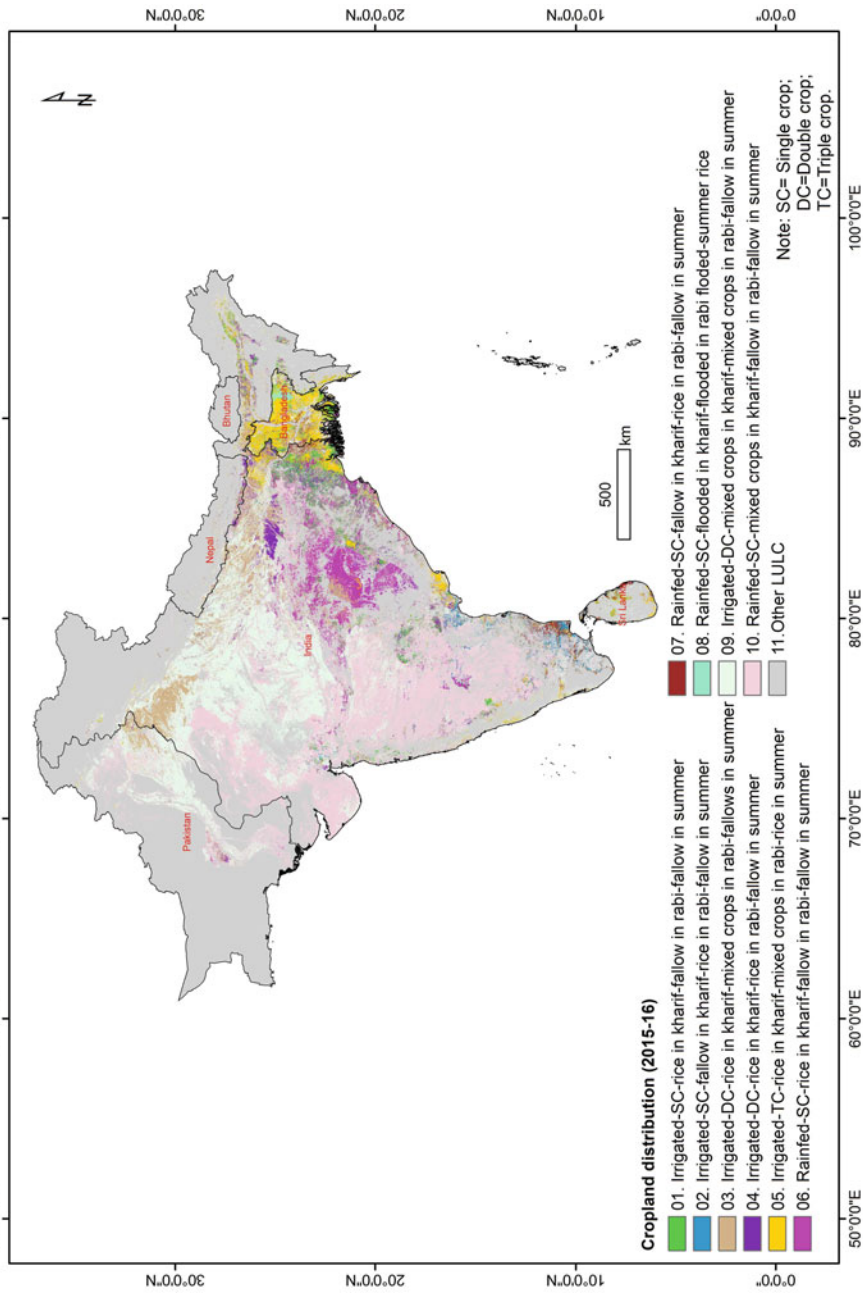

Fig. 21.4 Spatial distribution of land use/land cover in South Asia for the years 2015–2016

21.4.2 Spatiotemporal Distribution of Rice Fallows

The temporal changes in rice fallow area of South Asia over 10 years from 2005–2006 to 2015–2016 fallow extent areas are shown in Fig. 21.5. Rice classes identified based on ground survey data include GPS-referenced digital images, and temporal NDVI signatures for each of the rice classes are shown in Thenkabail et al. (2007) and Gumma et al. (2011b). Altogether, eight rice classes were identified and labeled in various ecoregions (Fig. 21.4). Figure 21.5 shows rabi fallows along with other croplands and non-cropland areas (Table 21.3).

The irrigated area estimated using the LULC map is 106 Mha in South Asian region, which is 58% of total agriculture area (Table 21.2). When compared with national statistics, MODIS-derived irrigated area was 15% higher. MODIS net rainfed agriculture was calculated as 84 Mha, which is 42% of total agriculture area. Finally irrigated area estimated using the map was compared against state-level irrigated area statistics available from national agencies. A good correlation was found with an R^2 of 0.93, and root-mean-square error (RMSE) was 859,000 ha (Fig. 21.6).

Accuracy was estimated using error matrices on resultant LULC classification (Table 21.4) with 568 ground surveyed points. Accuracy assessment was performed on resultant 11 classes. Out of 568 points, 463 locations matched with the resulted LULC classification. The overall accuracy of nine LULC classes was 81.5% and kappa value of 0.787.

21.4.3 Spatial Extent of Rice Fallows

Figure 21.4 illustrates the spatial extent of rice-growing areas derived from MOD13Q1.005 time series data with spectral matching techniques for the years 2015–2016. Three classes, namely, irrigated single crop *kharif* rice followed by fallow, irrigated double crop *kharif* rice followed by fallow summer rice, and rainfed single crop *kharif* rice followed by fallow summer fallow, were delineated as fallows after *kharif* rice. Rainfed rice areas were mainly located in the eastern and central parts of India, including the states of Chhattisgarh, Madhya Pradesh, Odisha, Jharkhand, and West Bengal. Significant parts in Sri Lanka also grow rainfed rice. Rainfed with supplemental irrigated areas are mainly located in the eastern part of India, including West Bengal and parts of Odisha adjacent to West Bengal. Irrigated rice systems are located in major irrigation command areas and also grown in double cropping system with rice followed by rice, rice followed by wheat, rice followed by other crops, and rice followed by fallows. The area under each of the three rice classes is shown in Table 21.3. Class names were assigned based on the above methodology, and each class specifies clearly rice crop during *kharif*. For example, class 1 "06 Rainfed single crop *kharif* rice fallows" full pixel area (FPA) is 12.17 Mha, which is dominated by rice along with other land cover areas, such as

Table 21.2 Rice systems in South Asia including other agriculture areas with irrigation source (crop year 2015–2016)

Class description	Full pixel area (FPA) (000′ ha)	% of total area (FPA)	Cropland fraction (%)			Actual cropland area (000′ ha)			Total gross cropland land area (000′ ha)
			Kharif	Rabi	Summer	Kharif	Rabi	Summer	
1. Irrigated SC rice in kharif fallow in rabi fallow in summer	6822	4.9	**96.1**	**8.1**	**3.2**	6556	553	218	7327
2. Irrigated SC fallow in kharif rice in rabi fallow in summer	2540	1.4	3.1	92.2	3.1	79	2342	79	2499
3. Irrigated DC rice in kharif-mixed crops in rabi fallows in summer	25,391	9.9	91	62.2	3.3	23,106	15,793	838	39,738
4. Irrigated DC rice in kharif rice in rabi fallow in summer	6823	1.3	96.3	86.6	3	6571	5909	205	12,685
5. Irrigated TC rice in kharif-mixed crops in rabi rice in summer	10,890	2.7	97.3	78.7	68.2	10,596	8570	7427	26,593
6. Rainfed SC rice in kharif fallow in rabi fallow in summer	12,171	6.8	**98.3**	**2.9**	**2.1**	11,965	353	256	12,573
7. Rainfed SC fallow in kharif rice in rabi fallow in summer	2983	0.4	3	93.6	3	89	2792	89	2971
8. Rainfed SC flooded in kharif flooded in rabi-flooded summer rice	543	0.3	3	3	91.9	16	16	499	532
9. Irrigated DC-mixed crops in kharif-mixed crops in rabi fallow in summer	73,490	35.0	86.7	83.2	3.5	63,715	61,143	2572	127,431
10. Rainfed SC-mixed crops in kharif fallow in rabi fallow in summer	77,375	37.3	77.7	18	0	60,120	13,927	0	74,048
Total croplands	219,029					182,814	111,400	12,183	306,397
Net cropland areas cultivated in South Asia, full pixel areas (FPA) = 219,029,000 ha									
Net cropland areas cultivated in South Asia, subpixel areas (SPAs) or actual areas during kharif season (June–October) = 182,814,000 ha									
Net cropland areas cultivated in South Asia, subpixel areas (SPAs) or actual areas during rabi season (November–February) = 111,400,000 ha									
Net cropland areas cultivated in South Asia, subpixel areas (SPAs) or actual areas during summer season (March–May) = 12,183,000 ha									

(continued)

Table 21.2 (continued)

Class description	Full pixel area (FPA) (000′ ha)	% of total area (FPA)	Cropland fraction (%)			Actual cropland area (000′ ha)			Total gross cropland land area (000′ ha)
			Kharif	Rabi	Summer	Kharif	Rabi	Summer	
Gross cropland areas cultivated in South Asia, subpixel areas (SPAs) or actual areas = 307,189,000 ha									
For classes 1 and 6 (Note: these two classes have rice during kharif and left fallow in rabi)									
Total net cultivated areas during kharif in South Asia, SPAs or actual areas of classes 1 and 6 = 18,520,789 ha									
Total net cultivated areas during rabi in South Asia, SPAs or actual areas of classes 1 and 6 = 905,579 ha									
Total uncultivated areas during rabi that were cultivated during kharif, SPAs or actual areas of classes 1 and 6 = 17,615,211 ha									

The table shows full pixel area (*FPA*), crop area fraction (*CAF*), and subpixel area (*SPA*) or actual area. SPA = FPA * CAF

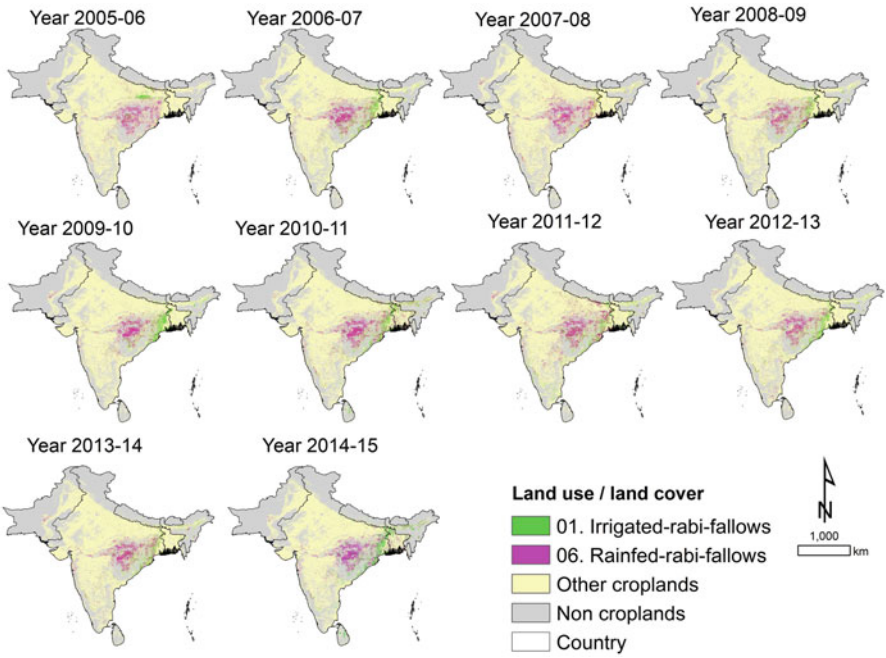

Fig. 21.5 Spatiotemporal distribution of rice fallows (rabi fallows)

Table 21.3 Net rice fallow in South Asia with irrigation source

Rice fallow (rabi fallow) classes	Rice fallows (000′ ha)	Percent of total rice fallows (%)
1. Irrigated SC rice in *kharif* fallow in *rabi* fallow in summer	6004	34
6. Rainfed SC rice in *kharif* fallow in *rabi* fallow in summer	11,612	66
Irrigated + rainfed rabi fallows + kharif rice: total	17, 615	100

trees, shrubs, grasses, water, fallows, and other crops. Rice fallows were mainly located in the central and eastern parts of India to a total of 17.6 Mha, which is 26% of total net rice-grown area in this region, which includes irrigated and rainfed areas. This means 26% of rice-growing area in South Asia is left fallow after growing rice in the rainy season. This elicits a large potential to intensify cropping in these lands based on the suitability. Subnation-wise rice fallows were shown in Table 21.5.

The rice estimates derived from the map generated in this study were compared against seasonal rice area statistics obtained from South Asian countries at the

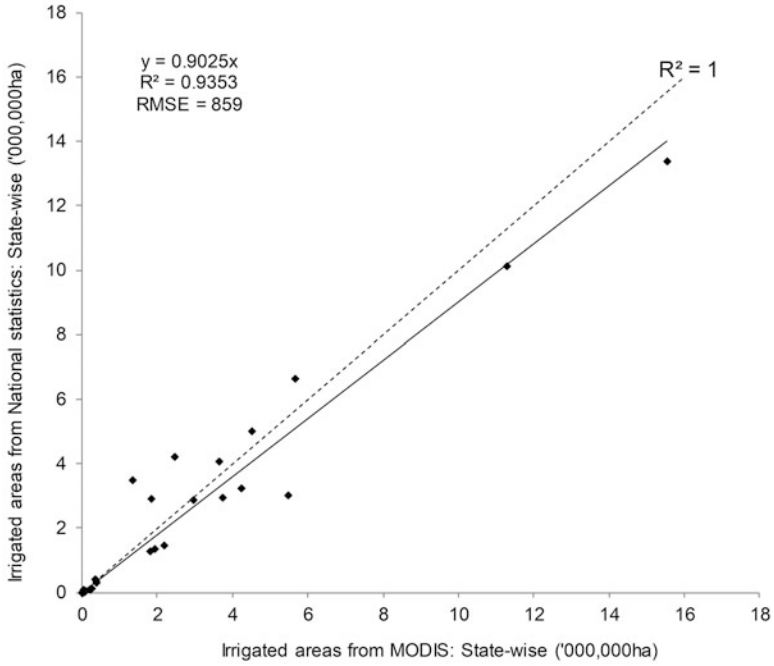

Fig. 21.6 The irrigated areas derived using MODIS 250 m imagery compared with agricultural census data for 2013–2014 (Administrative boundaries shown in Fig. 21.1b)

district level. Data was obtained for 840 administrative districts. The MODIS-derived rice areas were consistently nearer to the official estimates in all districts (Fig. 21.7). The R^2 value is 0.84 and RMSE was 40,079 ha (Fig. 21.7). The overestimation is obvious in 1:1 plot (Fig. 21.7). Present study clearly showed that statistical estimates can be generated at the district level from the thematic maps generated from satellite imagery.

21.4.4 Discussion on Methodology

The present research used MOD13Q1.005 temporal data to identify rice fallows with rice systems and irrigated areas across South Asia. MODIS captures imagery over the Earth on a daily basis, which makes it possible to get cloud-free data when available immediately after a rainfall event or cloudy day. The 16 day composites from the daily acquisitions bundle up to make a time series dataset over a crop year or a calendar year. This type of dataset provides temporal profiles of crop-growing locations to identify the start of season, peak growth stage, and harvest date during each season. The values of NDVI as function of time also help in identifying the type

Table 21.4 Accuracy assessment using error matrix (land-use/land cover classification)

Crop classification	I.	II.	III.	IV.	V.	VI.	VII	VIII	IX.	X.	XI.	Class totals	Reference totals	Classified totals	Users' accuracy (%)	Producers' accuracy (%)	Kappa
I. Irrigated SC rice in kharif fallow in rabi fallow in summer	21	0	0	1	1	0	0	0	0	0	0	24	46	37	91	88	0.909
II. Irrigated SC fallow in kharif rice in rabi fallow in summer	1	16	0	1	0	0	1	0	0	1	0	20	26	19	80	80	0.793
III. Irrigated DC rice in kharif-mixed crops in rabi fallows in summer	0	1	59	8	1	8	0	0	1	0	0	62	48	37	76	95	0.727
IV. Irrigated DC rice in kharif rice in rabi fallow in summer	0	0	1	20	2	3	0	0	1	0	0	37	55	49	74	54	0.723
V. Irrigated TC rice in kharif-mixed crops in rabi rice in summer	0	0	1	6	57	0	1	0	7	0	0	66	60	54	79	86	0.764
VI. Rainfed SC rice in kharif fallow in rabi fallow in summer	1	1	0	0	4	68	0	0	3	1	0	92	57	43	87	74	0.847

(continued)

Table 21.4 (continued)

Crop classification	I.	II.	III.	IV.	V.	VI.	VII	VIII	IX.	X.	XI.	Class totals	Reference totals	Classified totals	Users' accuracy (%)	Producers' accuracy (%)	Kappa
VII. Rainfed SC fallow in kharif rice in rabi fallow in summer	0	1	0	0	0	0	29	0	1	1	0	34	10	5	91	85	0.9
VIII. Rainfed SC flooded in kharif flooded in rabi-flooded summer rice	0	0	0	0	0	0	0	5	0	0	0	5	5	5	100	100	1
IX. Irrigated DC-mixed crops in kharif-mixed crops in rabi fallow in summer	0	0	0	0	0	1	0	0	87	5	1	110	115	88	93	79	0.908
X. Rainfed SC-mixed crops in kharif fallow in rabi fallow in summer	1	0	1	1	1	11	2	0	10	76	1	86	109	105	73	88	0.683
XI. Other LULC	0	1	0	0	0	1	1	0	0	2	30	32	37	21	86	94	0.849
Column total	45	21	40	58	74	62	12	7	102	122	25	568	568	463			
Overall classification Accuracy = 82% overall Kappa statistics = 0.79																	

Table 21.5 MODIS rice areas with rice fallows and subnational statistics at state wise (2015–2016)

Country	State	MODIS-derived areas ('000 ha)			Subnational statistics ('000 ha)
		Total net rice area	Rice fallows (rainfed)	Rice fallows (irrigated)	
Bangladesh	Barisal	528	49	147	987
Bangladesh	Chittagong	1001	29	104	1093
Bangladesh	Dhaka	2103	21	60	1303
Bangladesh	Khulna	1011	29	69	904
Bangladesh	Rajshahi	2479	25	161	2015
Bangladesh	Sylhet	725	33	75	456
Bhutan	Bhutan	128	7	13	NA
India	Andhra Pradesh	4266	618	690	2922
India	Arunachal Pradesh	326	16	75	122
India	Assam	2150	165	365	2139
India	Bihar	4501	223	188	3232
India	Chandigarh	2	0	0	NA
India	Chhattisgarh	5839	4099	87	5820
India	Dadra and Nagar Haveli	8	2	4	10
India	Daman and Diu	0	0	0	2
India	Delhi	3	1	0	NA
India	Goa	52	2	4	31
India	Gujarat	757	139	164	728
India	Haryana	817	5	1	1243
India	Himachal Pradesh	119	3	6	NA
India	Jammu and Kashmir	200	2	10	212
India	Jharkhand	2522	921	770	2440
India	Karnataka	1509	342	233	NA
India	Kerala	246	3	4	162
India	Lakshadweep	0	0	0	NA
India	Madhya Pradesh	4193	2018	213	1522
India	Maharashtra	1500	377	278	1486
India	Manipur	151	29	42	NA
India	Meghalaya	342	13	45	95
India	Mizoram	2	0	0	NA
India	Nagaland	19	0	1	165
India	Orissa	4484	1653	1012	3933
India	Pondicherry	23	0	0	4
India	Punjab	2525	5	1	2517

(continued)

Table 21.5 (continued)

Country	State	MODIS-derived areas ('000 ha)			Subnational statistics ('000 ha)
		Total net rice area	Rice fallows (rainfed)	Rice fallows (irrigated)	
India	Rajasthan	13	5	1	130
India	Sikkim	6	0	0	12
India	Tamil Nadu	2788	13	46	1906
India	Tripura	118	6	31	NA
India	Uttar Pradesh	5191	277	58	5632
India	Uttaranchal	212	4	9	270
India	West Bengal	5809	511	1138	NA
Nepal	Central	541	20	25	419
Nepal	East	561	17	42	419
Nepal	Far-Western	110	2	5	150
Nepal	Mid-Western	136	5	7	174
Nepal	West	354	7	8	335
Pakistan	Baluchistan	48	17	0	NA
Pakistan	F.C.T.	0	0	0	NA
Pakistan	Kashmir Pak	7	0	1	NA
Pakistan	Khyber	28	0	1	NA
Pakistan	Punjab Pak	1288	7	3	NA
Pakistan	Sind	374	51	4	NA
Pakistan	Tribal areas	7	0	0	NA
Sri Lanka	Central Sri	32	0	3	57
Sri Lanka	Eastern	209	1	9	89
Sri Lanka	North Central	213	1	20	78
Sri Lanka	North Western	32	0	1	25
Sri Lanka	Northern	107	1	2	265
Sri Lanka	Sabaragamuwa	17	0	0	34
Sri Lanka	Southern	138	1	1	33
Sri Lanka	Uva	119	1	3	91
Sri Lanka	Western	19	0	0	57

of crop in an ecoregion based on certain peak thresholds for that crop. This study applies spectral matching technique which is found to be ideal in mapping irrigated areas (Thenkabail et al. 2007) and mapping rice areas (Gumma et al. 2011a, b, c, d). Mapping spatial distribution of rice fallows using MODIS 250 m 16 day time series and ground survey information with spectral matching techniques is a significant new advancement in the use of this technique.

Some discrepancies were also found during the comparison of national statistics and MODIS-derived irrigated areas. The mismatch occurred in high-rainfall zones, where there was misclassification with irrigated areas due to similar growing

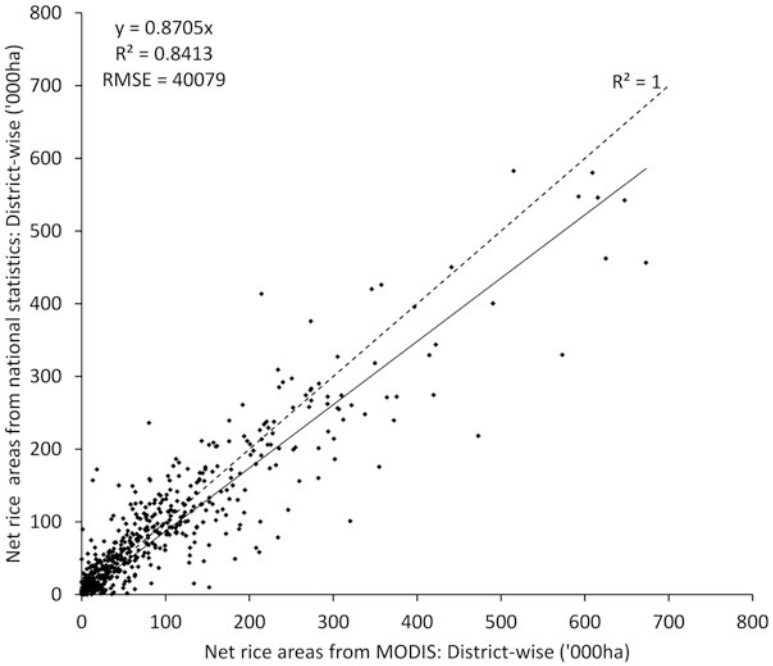

Fig. 21.7 The rice areas derived using MODIS 250 m compared with agricultural census data for 2010–2011 (Gumma et al. 2016) (Administrative boundaries in Fig. 21.1)

conditions during cropping season. Most of the areas were corrected using rainfall data and spatial modeling techniques.

Irrigated area fractions (the proportion of irrigated/rice area in a pixel) were assigned based on land-use proportions in each class to estimate the MODIS pixel area accurate to the real irrigated/rice area. Also, this method relies on ground survey information that is a truly representative sample of the fragmented rice systems. Higher-resolution imagery could be used to provide a more accurate estimate of pure classes but with a lot more mixed classes coming up. Results clearly show that present methods and MODIS time series data have many advantages such as capturing large-scale cropping pattern. But to minimizing errors, additional research will be attempted with multi-sensor images with advanced fusion techniques (Gumma et al. 2011c).

21.4.5 Discussion on Rice Fallows and Rice-Growing Areas

Mapping rice fallow is very important for the promotion of short-duration legumes for sustainable intensification and improving livelihoods. Rice fallow areas are high-

rainfall zones during the monsoon season (Ali et al. 2014; Satyanarayana et al. 1997), and soils have significant residual soil moisture to grow a short-duration legume crop after monsoon rice. An important reason for fallowing these lands is the scarcity of water for a normal crop like rice, etc. to be grown during the post-rainy season (*rabi*). Accurate up-to-date spatial distribution of rice fallows and statistics are important to guide breeders and policymakers to promote short-duration crops in this region. Soil-water availability and phenological information will inform breeders to select appropriate variety in a region.

21.5 Conclusions

The present study demonstrated the methodology adopted for mapping rice fallow along with LULC including irrigated areas and rice systems over large areas. Also an estimated district-level extent of rice fallow will be made available in the public domain (maps.icrisat.org) for national departments and multidisciplinary teams to promote short-duration grain legumes for increasing cropping intensity in South Asian region. MODIS 250 m 16 day temporal images were used to identify rice fallows with suite of methods, such as spectral matching techniques and decision tree algorithms. The results were validated with extensive ground survey information. MODIS-derived rice areas at the district level were compared with national statistics. The R^2 value was 0.84, and root-mean-square error was 40,079 ha with 735 district administrative boundaries. MODIS-derived net rice cropped area is 56,940,000 ha, which is slightly higher than national statistics (55,139,300 ha). The total area under rice fallow in South Asia is 16,808,960 ha including in rainfed and irrigated environments. In rainfed environment, it is 14,380,250 ha, and in irrigated environment, it is 2,427,713 ha. Accuracy assessment was performed by error matrix with ground survey information, and overall accuracy is 75% with kappa coefficient of 0.644. Present methods and approaches are found to be ideal for mapping rice systems with rice fallows in over larger areas in South Asia. District-wise spatial extent of rice fallows and irrigated areas will guide breeders and social scientists to promote short-duration grain legumes. The research creates a broad contribution to the methods and products of the Group on Earth Observations (GEO) for monitoring agriculture areas, Agriculture and Water Societal Beneficial Areas (GEO Agriculture and Water SBAs), the GEO Global Agricultural Monitoring Initiative (GEO GLAM), the global cropland area database using Earth observation data, and studies pertaining to global croplands, their water use, and food security in the twenty-first century (https://powellcenter.usgs.gov/globalcroplandwater/). The information on these types of domains needs to be updated regularly to guide the decision-makers and agricultural scientists to plan for sustained food production for food and nutrition security.

Acknowledgments This research was supported by two CGIAR Research Programs: Grain Legumes and Dryland Cereals (GLDC) and (Water Land and Ecosystems (WLE)). The research

was also supported by the global food security support analysis data at 30 m project (GFSAD30; http://geography.wr.usgs.gov/science/croplands/; https://croplands.org/) funded by the NASA MEaSUREs (Making Earth System Data Records for Use in Research Environments) funding obtained through NASA ROSES solicitation as well as by the Land Change Science (LCS), Land Remote Sensing (LRS), and Climate Land Use Change Mission Area Programs of the US Geological Survey (USGS). The authors would like to thank to the International Rice Research Institute (IRRI) for providing ground survey data and district-wise national statistics; Dr. Dheeravath Venkateshwarlu, Dr. Andrew Nelson, and Dr. Mitch Scull for supporting ground surveys in India; Dr. Saidul Islam for Bangladesh ground survey data and Dr. Nimal Desanayake for Sri Lanka ground survey data. Also thanks to Ms. Deepika Uppala for supporting data analysis.

References

Alexandratos N, Bruinsma J (2012) World agriculture towards 2030/2050: the 2012 revision. http://large.stanford.edu/courses/2014/ph240/yuan2/docs/ap106e.pdf. Accessed in 08 June 2015. ESA working paper 3

Ali M, Ghosh P, Hazra K (2014) Resource conservation technologies in rice fallow. Resource conservation technology in pulses, First edited by PK Ghosh, N Kumar, MS Venkatesh, KK Hazra, N Nadarajan, 01/2014: chapter 7: pp 83–88, Scientific publishers, ISBN: 978-81-7233-885-5

Badhwar GD (1984) Automatic corn-soybean classification using landsat MSS data. I. Near-harvest crop proportion estimation. Remote Sens Environ 14(1–3):15–29

Biggs TW, Thenkabail PS, Gumma MK, Scott CA, Parthasaradhi GR, Turral HN (2006) Irrigated area mapping in heterogeneous landscapes with MODIS time series, ground truth and census data, Krishna Basin, India. Int J Remote Sens 27(19):4245–4266

Biradar CM, Thenkabail PS, Noojipady P, Li Y, Dheeravath V, Turral H, Velpuri M, Gumma MK, Reddy GPO, Cai XL, Xiao X, Schull MA, Alankara RD, Gunasinghe S, Mohideen S (2009) A global map of rainfed cropland areas (GMRCA) at the end of last millennium using remote sensing. Int J Appl Earth Obs Geoinf 11(2):114–129

Choice H (2009) Agroecological zones. Available http://harvestchoice.org/production/biophysical/agroecology. Downloaded 01/05/ 2010

Cihlar J, Xiao Q, Chen J, Beaubien J, Fung K, Latifovic R (1998) Classification by progressive generalization: A new automated methodology for remote sensing multichannel data. Int J Remote Sens 19(14):2685–2704

Congalton RG (2001) Accuracy assessment and validation of remotely sensed and other spatial information. Int J Wildland Fire 10(4):321–328

Dheeravath V, Thenkabail PS, Chandrakantha G, Noojipady P, Reddy GPO, Biradar CM, Gumma MK, Velpuri M (2010) Irrigated areas of India derived using MODIS 500 m time series for the years 2001–2003. ISPRS J Photogramm Remote Sens 65(1):42–59

FAO (2015) FAOSTAT. http://faostat.fao.org/. Accessed on 02 June 2015

Fischer A (1994) A model for the seasonal variations of vegetation indices in coarse resolution data and its inversion to extract crop parameters. Remote Sens Environ 48(2):220–230

Garnett T, Appleby M, Balmford A, Bateman I, Benton T, Bloomer P, Burlingame B, Dawkins M, Dolan L, Fraser D (2013) Sustainable intensification in agriculture: premises and policies. Science 341(6141):33–34

Gray J, Friedl M, Frolking S, Ramankutty N, Nelson A, Gumma M (2014) Mapping Asian cropping intensity with MODIS. Sel Top Appl Earth Obs Remote Sens IEEE J PP 99:1–7

Gumma MK, Gauchan D, Nelson A, Pandey S, Rala A (2011a) Temporal changes in rice-growing area and their impact on livelihood over a decade: a case study of Nepal. Agric Ecosyst Environ 142(3–4):382–392

Gumma MK, Nelson A, Thenkabail PS, Singh AN (2011b) Mapping rice areas of South Asia using MODIS multitemporal data. J Appl Remote Sens 5:053547

Gumma MK, Thenkabail PS, Hideto F, Nelson A, Dheeravath V, Busia D, Rala A (2011c) Mapping irrigated areas of Ghana using fusion of 30 m and 250 m resolution remote-sensing data. Remote Sens 3(4):816–835

Gumma MK, Thenkabail PS, Muralikrishna IV, Velpuri MN, Gangadhararao PT, Dheeravath V, Biradar CM, Acharya Nalan S, Gaur A (2011d) Changes in agricultural cropland areas between a water-surplus year and a water-deficit year impacting food security, determined using MODIS 250 m time-series data and spectral matching techniques, in the Krishna River basin (India). Int JRemote Sens 32(12):3495–3520

Gumma MK, Thenkabail PS, Maunahan A, Islam S, Nelson A (2014) Mapping seasonal rice cropland extent and area in the high cropping intensity environment of Bangladesh using MODIS 500m data for the year 2010. ISPRS J Photogramm Remote Sens 91(5):98–113

Gumma MK, Kajisa K, Mohammed IA, Whitbread AM, Nelson A, Rala A, Palanisami K (2015a) Temporal change in land use by irrigation source in Tamil Nadu and management implications. Environ Monit Assess 187(1):1–17

Gumma MK, Mohanty S, Nelson A, Arnel R, Mohammed IA, Das SR (2015b) Remote sensing based change analysis of rice environments in Odisha, India. J Environ Manag 148:31–41

Gumma MK, Thenkabail PS, Teluguntla P, Rao MN, Mohammed IA, Whitbread AM (2016) Mapping rice-fallow cropland areas for short-season grain legumes intensification in South Asia using MODIS 250 m time-series data. Int J Digital Earth 9(10):981–1003

Homayouni S, Roux M (2003) Material mapping from hyperspectral images using spectral matching in urban area. In: Landgrebe P (ed) IEEE Workshop in honour of Prof. Landgrebe, Washington DC, USA, October 2003

INDIASTAT (2015) State-wise net area irrigated by source in India and state-wise irrigated area under crops in India. www.indiastat.com. Accessed in 30 May 2015

Jensen JR (2004) IIntroductory digital image processing: a remote sensing perspective, 3rd edn. Upper Saddle River, Prentice Hall, p 544

Knight JF, Lunetta RL, Ediriwickrema J, Khorram S (2006) Regional scale land-cover characterization using MODIS-NDVI 250 m multi-temporal imagery: a phenology based approach. GISci Remote Sens 43(1):1–23

Lobell DB, Asner GP, Ortiz-Monasterio JI, Benning TL (2003) Remote sensing of regional crop production in the Yaqui Valley, Mexico: estimates and uncertainties. Agric Ecosyst Environ 94(2):205–220

LPDAAC (2014) The land processes distributed active archive center – See more at: https://lpdaac.usgs.gov/#sthash.MxeroLVs.dpuf. Accessed on 15 April 2014

Sakamoto T, Yokozawa M, Toritani H, Shibayama M, Ishitsuka N, Ohno H (2005) A crop phenology detection method using time-series MODIS data. Remote Sens Environ 96(3–4):366–374

Satyanarayana A, Seenaiah P, Sudhakara Babu K, Prasada Rao M (1997) Extending pulses area and production in rice fallow. In: Asthana AN, Ali M (eds) Recent advances in pulses research. Indian Society of Pulses Research and Development, Indian Institute of Pulses Research, Kanpur, pp 569–580

Shao Y, Fan X, Liu H, Xiao J, Ross S, Brisco B, Brown R, Staples G (2001) Rice monitoring and production estimation using multitemporal RADARSAT. Remote Sens Environ 76(3):310–325

Subbarao G, KumarRao J, Kumar C, Johansen U, Irshad A, KrishnaRao L, Venkataratnam K, Hebbar K, Sai M, Harries D (2001) Spatial distribution and quantification of rice-fallows in south Asia: potential for legumes. ICRISAT, Patancheru, p 316 ICRISAT

Thenkabail PS (2010) Global croplands and their importance for water and food security in the twenty-first century: towards an ever green revolution that combines a second green revolution with a blue revolution. Remote Sens 2(9):2305–2312

Thenkabail PS, Schull M, Turral H (2005) Ganges and Indus river basin land use/land cover (LULC) and irrigated area mapping using continuous streams of MODIS data. Remote Sens Environ 95(3):317–341

Thenkabail P, GangadharaRao P, Biggs T, Gumma M, Turral H (2007) Spectral matching techniques to determine historical land-use/land-cover (LULC) and irrigated areas using time-series 0.1-degree AVHRR pathfinder datasets. Photogramm Eng Remote Sens 73(10):1029–1040

Thenkabail PS, Biradar CM, Noojipady P, Dheeravath V, Li YJ, Velpuri M, Reddy G, Cai X, Gumma M, Turral H (2008) A global irrigated area map (GIAM) using remote sensing at the end of the last millennium. International Water Management Institute, Colombo

Thenkabail P, Biradar C, Noojipady P, Dheeravath V, Li Y, Velpuri M, Gumma M, Reddy GPO, Turral H, Cai X, Vithanage J, Schull M, Dutta R (2009) Global irrigated area map (GIAM) derived from remote sensing, for the end of last millennium. Int J Remote Sens 30(14):3679–3733

Thiruvengadachari S, Sakthivadivel R (1997) Satellite remote sensing for assessment of irrigation system performance: a case study in India, Research report 9. International Irrigation Management Institute, Colombo

Tou JT, Gonzalez RC (1975) Pattern recognition principles. Addison-Wesley Publishing Company, Reading

USDA (2010) United States department of agriculture. foreign agricultural service. www.fas.usda.gov/psdonline/. Accessed on 21 May 2015. USDA

Velpuri NM, Thenkabail PS, Gumma MK, Biradar CB, Noojipady P, Dheeravath V, Yuanjie L (2009) Influence of resolution in irrigated area mapping and area estimations. Photogramm Eng Remote Sens 75(12):1383–1395

World Bank (2015) PovcalNet. http://iresearch.worldbank.org/PovcalNet/povcalNet.html. Accessed on 25 May 2015